Model-Independent Time-Resolved Fluorescence Depolarization from Ordered Biological Assemblies Applied to Restricted Motion of Myosin Cross-Bridges in Muscle Fibers†

Thomas P. Burghardt* and Katalin Ajtai‡
Cardiovascular Research Institute, University of California, San Francisco, San Francisco, California 94143
Received October 22, 1985; Revised Manuscript Received January 7, 1986

ABSTRACT: We formulate a model-independent description of time-dependent restricted molecular rotational motion and apply it to the time-resolved fluorescence depolarization signal from fluorescence-labeled molecules following polarized excitation. In this treatment, the time-dependent molecular orientation distribution is equal to the operation of a linear time-development operator on the initial orientation distribution. The formula for the time-development operator is derived from the equation of motion for the orientation distribution. The time-development operator is then expanded in time in terms of a complete set of orthonormal polynomials. When this expression for the orientation distribution is used to calculate the time-resolved fluorescence depolarization signal, properties of the orthonormal polynomials allow the signal to be quantitated uniquely in terms of matrix elements of the differential operators from the equation of motion. We demonstrate how to obtain the experimental value of the matrix elements directly from the fluorescence depolarization signal. In this paper, we also describe the application of the model-independent formalism to fluorescence-labeled myosin cross-bridges in muscle fibers when the fibers are in a variety of physiological states. We show that the analysis of time-resolved fluorescence depolarization data with the new formalism and the rotational diffusion in a potential model results in a slight revision of our previous estimate of the relaxed cross-bridge rotational diffusion constant and the determination of rank 6 order parameters that were ignored in the previous analysis [Burghardt, T. P., & Thompson, N. L. (1985) *Biochemistry 24*, 3731–3735]. The rank 6 order parameters are shown to make a significant contribution to the proposed steady-state angular distribution of the relaxed cross-bridges. Order parameters of rank 6 do not contribute to the steady-state fluorescence polarization signal and can only be detected with the time-resolved signal [Burghardt, T. P. (1984) *Biopolymers 23*, 2383–2406]. We have also applied the model-independent formalism to new data from fibers in rigor when the fibers are in a configuration such that the excitation light polarization is perpendicular to the fiber axis and the light propagates along the fiber axis, so that the fluorescence depolarization signal is sensitive to probe rotational motions about the fiber axis. We show that in this configuration the rigor cross-bridge is undergoing rapid rotational motion, probably due to conjugate motion in the actin filament, with a rate that is not significantly affected by the presence of calcium or when the fiber is decorated with extrinsic subfragment 1 of myosin.

Time-resolved fluorescence depolarization following polarized excitation is employed to study the nanosecond rotational motion of elementary subunits of biological assemblies. In this technique, the elemental subunits are specifically labeled with a fluorescent probe. Following a brief flash of polarized excitation light, the dipolar fluorescent emission of the probes is detected as a function of time and the emission polarization. The calculation of the time course of the polarized fluorescent emission includes the effects of the finite lifetime and the nanosecond rotational motion of the probe.

Usually the calculation of the time course of the emission decay from rotational motion of the probe is done by using a suitable model for the probe motion. The models generally used are rotational diffusion (Favro, 1960; Ehrenberg & Rigler, 1972; Chuang & Eisenthal, 1972) and rotational diffusion in a potential (Kinosita et al., 1977; Szabo, 1980; Zannoni et al., 1983). Similar calculations have been performed to determine the effect of probe motion on the shape of electron spin resonance spectra (McCalley et al., 1972; Polnaszek et al., 1973). Recently we have described a calculation of the time-resolved fluorescence depolarization signal for rotational diffusion in a general model-independent potential (Burghardt, 1985; Burghardt & Thompson, 1985a). In the present paper, we describe a new method of calculation for the time course of the emission decay that accounts for the rotational motion of the probe in a completely model-independent way.

With model-independent time-resolved fluorescence depolarization, the time development of the angular distribution function, P, is obtained by using a linear, time-development operator, T, such that $P(t) = T(t,t_0)P(t_0)$ when $t > t_0$. The mathematical formula of T is determined from the equation of motion of $P(t)$. T is then expanded in time in a complete set of orthogonal polynomials. The coefficients of the expansion are terms with increasing order in the differential operator that makes up T and that describes the physical process causing the molecular rotational motion. When this expression for $P(t)$ is used to calculate the time-resolved fluorescence depolarization signal, properties of the orthonormal polynomials allow the matrix elements of the expansion coefficients to be determined directly from the fluorescence depolarization data. Because we need not explicitly specify T, experimental results are tabulated in their most general form and can be interpreted without a model. Any model can

† This work was supported by U.S. Public Health Service Grant HL-16683, by a grant from the Muscular Dystrophy Association, and by American Heart Association Grant CI-8.
‡ Permanent address: Department of Biochemistry, Eötvös Loránd University, Budapest, Hungary.

0006-2960/86/0425-3469$01.50/0

be readily adapted to this formalism.

We have performed a model calculation of rotational diffusion in a three-dimensional angular potential. The model is used in interpreting fluorescence depolarization data from 5-[[[(iodoacetyl)amino]ethyl]amino]naphthalene-1-sulfonic acid (1,5-IAEDANS)-labeled cross-bridges in relaxed muscle fibers. An earlier model-dependent analysis of some of this data using a more conventional procedure (Burghardt & Thompson, 1985a; Burghardt, 1985) is shown to be in qualitative agreement with our new model-independent analysis. Quantitatively, the two methods are identical except in their estimates of the cross-bridge diffusion constants which differ by a factor of 2.

The model calculation is now applied to relaxed fibers in two geometrical configurations. In the vertical fiber configuration, the fiber axis is aligned with the excitation light polarization, and in the horizontal configuration, the fiber axis is rotated to be 90° from the excitation light polarization and 45° to the excitation light propagation direction. By requiring the model to account for the relaxation rates of the cross-bridges in both fiber configurations, we have acquired a new constraint on the free parameters in the model and consequently have been able to estimate experimental values of rank 6 order parameters. The rank 6 order parameters contribute significantly to the proposed steady-state cross-bridge angular distribution, making it bimodal as a function of the polar angle measured relative to the fiber axis. Values of order parameters of rank >4 cannot be determined from steady-state measurements (Burghardt, 1984). The model calculation for relaxed fibers is the first reported model calculation using a three-dimensional angular potential. A symbolic manipulation computer program was used for the extensive algebraic manipulations in the model calculation.

We have also performed new experiments on muscle fibers in rigor. We have shown previously that 1,5-IAEDANS-labeled cross-bridges in rigor show restricted rotational motion such that the cross-bridge rotates about an axis parallel to the fiber axis but not about axes perpendicular to the fiber axis (Burghardt & Thompson, 1985a). The distinction of the axes of rotation was achieved by comparison of fluorescence depolarization data from rigor fibers in the vertical and horizontal configurations. The motion detected in the horizontal fibers is rapid (200–300-ns anisotropy relaxation time) and is apparently caused by conjugate actin motion. Experiments reported here show that the rapidity of the motion is not significantly affected by the presence of calcium or when the thin filament is completely saturated with intrinsic myosin and unlabeled extrinsic subfragment 1 (S-1).

Theory

Equation of Motion. The equation of motion for molecular rotational motion is

$$-\frac{\partial}{\partial t}P(\Omega,t) = HP(\Omega,t) \tag{1}$$

where t is time, Ω represents the three Euler angles α, β, and γ describing the orientation of a coordinate system in space, H is an operator (that is not necessarily self-adjoint under the appropriate boundary conditions), and $P(\Omega,t)$ is the probability density for molecular orientations. If H is not explicitly dependent on time, eq 1 is separable in time and space coordinates so that

$$P(\Omega,t) = \exp[-H(t - t_0)]P(\Omega,t_0) \tag{2}$$

is the solution to eq 1 when $t > t_0$. The operator $\exp[-H(t - t_0)]$ is the time-development operator, denoted here by T.

The initial condition, determined by the experimental application, is expressed in the expanded form

$$P(\Omega,t_0) = \sum_{l,m,n} p_{l,m,n}\sqrt{\frac{2l+1}{8\pi^2}}D^l_{m,n}(\Omega) \tag{3}$$

where $D^l_{m,n}(\Omega)$ represents Wigner rotation matrix elements. These matrix elements obey an orthogonality rule such that (Davydov, 1963)

$$\int_{\Omega_0} d\Omega D^{*l'}_{m',n'}(\Omega)D^l_{m,n}(\Omega) = \frac{8\pi^2}{2l+1}\delta_{l',l}\delta_{m',m}\delta_{n',n} \tag{4}$$

where an asterisk means complex conjugate, Ω_0 is the domain $0 \le \alpha \le 2\pi$, $0 \le \beta \le \pi$, and $0 \le \gamma \le 2\pi$, and $\delta_{i,j}$ is the Kronecker delta. Using eq 3 and 4, we find

$$p_{l,m,n} = \sqrt{\frac{2l+1}{8\pi^2}}\int_{\Omega_0} d\Omega D^{*l}_{m,n}(\Omega)P(\Omega,t_0) \tag{5}$$

Application to Time-Resolved Fluorescence Depolarization. In a time-resolved fluorescence depolarization experiment, the intensity emitted by fluorophores specifically attached to elements of the biological assembly is observed. This intensity is the projection of $[\mathbf{v}(\chi)\cdot\boldsymbol{\mu}_e]^2$ onto $P(\Omega,t)$, where $\mathbf{v}(\chi)$ is a unit vector in the direction of polarization along which the emitted light is observed, χ is its angle from the lab frame z axis, and $\boldsymbol{\mu}_e$ is the unit electric dipole moment for emission of the fluorophore. When we express $\mathbf{v}$ in a spherical basis using the transformations

$$\begin{aligned} v^1 &= -(1/2)^{1/2}(v_x + iv_y) \qquad v^0 = v_z \\ v^{-1} &= (1/2)^{1/2}(v_x - iv_y) \end{aligned} \tag{6}$$

and in terms of lab frame coordinates using

$$v^m_{\text{mol}} = \sum_{m'} D^{*1}_{m',m}v^{m'}_{\text{lab}} \tag{7}$$

where subscripts "mol" and "lab" refer to molecule and laboratory fixed coordinates, we find

$$[\mathbf{v}(\chi)\cdot\boldsymbol{\mu}_e]^2 = \sum_{j=0}^{2}\sum_{\substack{m,m'\\n,n'}}(-1)^{m'+n'}\mu_e^{-m}\mu_e^{-n}S^{m',n'}D^{*j}_{m'+n',m+n}(\Omega) \tag{8}$$

$$\times(2j+1)\begin{pmatrix} 1 & 1 & j \\ m' & n' & -m'-n' \end{pmatrix}\begin{pmatrix} 1 & 1 & j \\ m & n & -m-n \end{pmatrix}$$

where

$$\begin{aligned} S^{m',n'} = {} & K_a v_1^{m'}v_1^{n'} + (K_b\cos^2\chi + \\ & K_c\sin^2\chi)v_2^{m'}v_2^{n'} + (K_b\sin^2\chi + K_c\cos^2\chi)v_3^{m'}v_3^{n'} + \\ & 2(K_c - K_b)\sin\chi\cos\chi\, v_2^{m'}v_3^{n'} \end{aligned} \tag{9}$$

and

$$\begin{pmatrix} j_1 & j_2 & j \\ m_1 & m_2 & m \end{pmatrix}$$

are Wigner $3-j$ symbols (Davydov, 1963). Constants K_a, K_b, and K_c in eq 9 are related to the numerical aperture of the collection optics for emitted light polarized in the x, y, and z directions of the lab frame (Axelrod, 1979; Burghardt & Thompson, 1984). The unit vectors $\mathbf{v}_1$, $\mathbf{v}_2$, and $\mathbf{v}_3$ in eq 9 point along the x, y, and z axes in the lab frame. In obtaining eq 8, we have used the relation for Wigner rotation matrix elements:

$$D^{j_1}_{m_1,k_1}(\Omega)D^{j_2}_{m_2,k_2}(\Omega) = \sum_{j=|j_1-j_2|}^{j_1+j_2}(-1)^{m+k}(2j+1)D^j_{m,k}(\Omega) \tag{10}$$

$$\times \begin{pmatrix} j_1 & j_2 & j \\ m_1 & m_2 & -m \end{pmatrix} \begin{pmatrix} j_1 & j_2 & j \\ k_1 & k_2 & -k \end{pmatrix}$$

The observed fluorescence signal following an excitation pulse of infinitesimal duration is (using eq 3, 4, and 8)

$$F(t) = F_0 \exp(-t/\tau) \int_{\Omega_0} d\Omega [\mathbf{v}(\chi)\cdot\mu_e]^2 P(\Omega,t) =$$

$$F_0 \exp(-t/\tau) \sum_{l,m,n} \sqrt{\frac{2l+1}{8\pi^2}}\, p_{l,m,n}[(1/3)(K_a + K_b + K_c) T_{0,0,0;l,m,n} + S^{1,1} U_{2,2;l,m,n}(T) + (1/2)^{1/2} S^{1,0} U_{2,1;l,m,n}(T) + (1/6)^{1/2}(S^{0,0} + S^{1,-1}) U_{2,0;l,m,n}(T)] \quad (11a)$$

where τ is the fluorescence lifetime of the probe and

$$U_{2,i;l,m,n}(T) = \mu_e^{1}\mu_e^{1}(T_{2,i,-2;l,m,n} + T_{2,-i,-2;l,m,n}) + \mu_e^{-1}\mu_e^{-1}(T_{2,i,2;l,m,n} + T_{2,-i,2;l,m,n}) - 2^{1/2}\mu_e^{1}\mu_e^{0}(T_{2,i,-1;l,m,n} + T_{2,-i,-1;l,m,n}) - 2^{1/2}\mu_e^{0}\mu_e^{-1}(T_{2,i,1;l,m,n} + T_{2,-i,1;l,m,n}) + (2/3)^{1/2}(\mu_e^{1}\mu_e^{-1} + \mu_e^{0}\mu_e^{0})(T_{2,i,0;l,m,n} + T_{2,-i,0;l,m,n}) \quad (11b)$$

The term $F_0 \exp(-t/\tau)$ in eq 11a accounts for the amplitude and time dependence of the signal due to the fluorescence lifetime. The symbol $T_{i,j,k;l,m,n}$ is the matrix element

$$T_{i,j,k;l,m,n} \equiv \int_{\Omega_0} d\Omega D^{*i}_{j,k}(\Omega) T D^{l}_{m,n}(\Omega) \quad (12a)$$

$$T_{i,j,k;l,m,n} = \int_{\Omega_0} d\Omega D^{*i}_{j,k}(\Omega) \exp(-Ht) D^{l}_{m,n}(\Omega) \quad (12b)$$

The time dependence in eq 11a is contained in the term $\exp(-t/\tau)T_{i,j,k;l,m,n}$. When $^1/_2\tau H < 1$, it is appropriate to expand $T_{i,j,k;l,m,n}$ in Laguere polynomials, $L_r(2t/\tau)$, such that (Abramowitz & Stegun, 1972)

$$\exp(-t/\tau)T_{i,j,k;l,m,n} = \exp(-t/\tau) \times \left\{ L_0(2t/\tau) \sum_{q=0}^{\infty} [(-\tfrac{1}{2}\tau H)^q]_{i,j,k;l,m,n} - L_1(2t/\tau) \sum_{q=1}^{\infty} q[(-\tfrac{1}{2}\tau H)^q]_{i,j,k;l,m,n} + \ldots + (-1)^r L_r(2t/\tau) \sum_{q=r}^{\infty} \frac{q!}{r!(q-r)!} [(-\tfrac{1}{2}\tau H)^q]_{i,j,k;l,m,n} + \ldots \right\} \quad (13)$$

When $^1/_2\tau H \gtrsim 1$, a similar expansion is performed. This procedure is described in the Appendix. The functions defined by

$$\phi_n \equiv (2/\tau)^{1/2} \exp(-t/\tau) L_n(2t/\tau) \quad (14)$$

are orthonormal on the interval $0 \le t < \infty$ such that

$$\int_0^{\infty} dt \phi_n(t)\phi_m(t) = \delta_{n,m} \quad (15)$$

We will show in the next section that the orthogonality of $\phi_n(t)$'s allows us to uniquely distinguish terms in the series of eq 13 that make up a fluorescence depolarization curve. The sums over q in eq 13 can be written in closed form as

$$(2/\tau)^{1/2} \exp(-t/\tau) T_{i,j,k;l,m,n} = \phi_0(2t/\tau) \left(\frac{1}{1 + \tfrac{1}{2}\tau H} \right)_{i,j,k;l,m,n} + \phi_1(2t/\tau) \left[\frac{\tfrac{1}{2}\tau H}{(1 + \tfrac{1}{2}\tau H)^2} \right]_{i,j,k;l,m,n} + \ldots + \phi_r(2t/\tau) \left[\frac{(\tfrac{1}{2}\tau H)^r}{(1 + \tfrac{1}{2}\tau H)^{r+1}} \right]_{i,j,k;l,m,n} + \ldots \quad (16)$$

Using eq 11 and operator O_r defined by

$$O_r \equiv \frac{(\tfrac{1}{2}\tau H)^r}{(1 + \tfrac{1}{2}\tau H)^{r+1}} \quad (17)$$

we find

$$F(t) \equiv F_0(\tau/2)^{1/2} \sum_{r=0}^{\infty} C_r \phi_r(2t/\tau) \quad (18a)$$

where

$$C_r = \sum_{l,m,n} p_{l,m,n} \sqrt{\frac{2l+1}{8\pi^2}} [(1/3)(K_a + K_b + K_c) \times (O_r)_{0,0,0;l,m,n} + S^{1,1} U_{2,2;l,m,n}(O_r) + (1/2)^{1/2} S^{1,0} U_{2,1;l,m,n}(O_r) + (1/6)^{1/2}(S^{0,0} + S^{1,-1}) U_{2,0;l,m,n}(O_r)] \quad (18b)$$

The coefficients $p_{l,m,n}$ are specified by the initial condition $P(\Omega,t=0)$, as shown by eq 5. In our application

$$P(\Omega,t=0) = P(\Omega,t\to\infty)[\mu_a\cdot\mathbf{E}(\epsilon)]^2 \quad (19)$$

where μ_a is the unit electric dipole moment for absorption, $\mathbf{E}(\epsilon)$ is the unit electric field vector of the excitation light, and ϵ is the angle vector $\mathbf{E}$ makes with the lab z axis. $P(\Omega,t\to\infty)$ is the steady-state angular distribution for molecular orientations and satisfies the steady-state equation $HP(\Omega,t\to\infty) = 0$.

The model-independent, steady-state angular distribution is

$$P(\Omega,t\to\infty) = \sum_{J,m_1,m_2} \sqrt{\frac{2J+1}{8\pi^2}}\, a^{J}_{m_1,m_2} D^{J}_{m_1,m_2}(\Omega) \quad (20)$$

Using eq 4–7 and 10 and an expression equivalent to eq 8 for $[\mathbf{E}(\epsilon)\cdot\mu_a]^2$, we find

$$p_{l,m,n} = (1/3)a^{l}_{m,n} + \sum_{J,k,q} \sqrt{\frac{2J+1}{2l+1}}\, a^{J}_{k,q}\{E^{-1}E^{-1}\langle J,2,k,2|l,m\rangle + E^{1}E^{1}\langle J,2,k,-2|l,m\rangle + (E^{0}E^{0} + E^{1}E^{-1})(2/3)^{1/2}\langle J,2,k,0|l,m\rangle - 2^{1/2}E^{0}E^{-1}\langle J,2,k,1|l,m\rangle - 2^{1/2}E^{1}E^{0}\langle J,2,k,-1|l,m\rangle\}\{\mu_a^{1}\mu_a^{1}\langle J,2,q,2|l,n\rangle + \mu_a^{-1}\mu_a^{-1}\langle J,2,q,-2|l,n\rangle + (\mu_a^{0}\mu_a^{0} + \mu_a^{1}\mu_a^{-1})(2/3)^{1/2}\langle J,2,q,0|l,n\rangle + 2^{1/2}\mu_a^{0}\mu_a^{-1}\langle J,2,q,-1|l,n\rangle + 2^{1/2}\mu_a^{0}\mu_a^{1}\langle J,2,q,1|l,n\rangle\} \quad (21)$$

Some of the order parameters $a^{l}_{m,n}$ in eq 21 can be determined from measurements with time-independent methods (Burghardt, 1984, 1985; Burghardt & Thompson, 1985a).

With eq 18, using eq 14, 17, and 21, the time-dependent fluorescence depolarization signal is constructed in a model-independent form. The unknown parameters are generally the matrix elements of the operator O_r. The linear combinations of these matrix elements, that are the coefficients C_r in eq 18b, are determined experimentally from time-resolved fluorescence depolarization curves. The method for experimental determination of C_r is demonstrated in the next section.

Determination of C_r from Real Time Resolved Fluorescence Depolarization Curves. In a real experiment, the excitation lamp pulse has a finite width that must be convoluted with the fluorescent emission signal $F(t)$ [see, for example, Badea & Brand (1979)]. Under these circumstances, it has been

shown that the observed signal, $\mathcal{F}(t)$, is

$$\mathcal{F}(t) = \int_0^t dt' F(t - t')\mathcal{L}(t') \quad (22)$$

where $\mathcal{L}(t)$ is the shape of the lamp pulse. Using eq 18a, we find

$$\mathcal{F}(t) = F_0(\tau/2)^{1/2}\sum_{r=0}^{\infty} C_r \int_0^t dt' \phi_r[2(t - t')/\tau]\mathcal{L}(t') \quad (23a)$$

$$\mathcal{F}(t) = F_0(\tau/2)^{1/2}\sum_{r=0}^{\infty} C_r g_r(2t/\tau) \quad (23b)$$

$g_r(t)$ is the new function of time in which the observed fluorescence signal is expanded. Unlike the $\phi_r(t)$'s, the $g_r(t)$'s are not orthogonal. The departure of the g_r's from orthogonality depends on the shape of the lamp pulse such that when the pulse is a δ function $g_r = \phi_r$. Using a general method described in detail previously (Burghardt & Thompson, 1985b), we numerically calculated the coefficients C_r from $\mathcal{F}(t)$ using the formula

$$C_r = \sum_{r'} G_{r,r'} \int_0^{\infty} dt g_{r'}(t)\mathcal{F}(t) \quad (24)$$

where $G_{r,r'}$ is an element of a matrix formed from the inverse of the matrix whose elements are $\int_0^{\infty} dt g_{r'}(t)g_r(t)$.

Application of the Formalism to a Real Time Resolved Instrument and to Fluorescent-Labeled Muscle Fibers. In our experimental application to myosin cross-bridges in muscle fibers, we employ low-aperture excitation and collection optics so that **E** is linearly polarized and $K_a = K_b = 0$. We choose **E** to be polarized along the lab z axis (corresponding to $\epsilon = 0$ in eq 19) so that **E** = (0,0,1). We simultaneously collect fluorescence polarized in the lab frame z and x axes (corresponding to $\chi = 0°$ and 90° in eq 8). Under these experimental conditions, the observed signals are

$$\mathcal{F}_{\parallel}(t) = \mathcal{F}(t,\epsilon=0,\chi=0) = F_0(\tau/2)^{1/2}\sum_{r=0}^{\infty} g_r(2t/\tau)C_r(\epsilon=0,\chi=0) \quad (25a)$$

$$\mathcal{F}_{\perp}(t) = \mathcal{F}(t,\epsilon=0,\chi=90°) = F_0(\tau/2)^{1/2}\sum_{r=0}^{\infty} g_r(2t/\tau)C_r(\epsilon=0,\chi=90°) \quad (25b)$$

where

$$C_r(\epsilon=0,\chi=0) = K_c \sum_{l,m,n} p_{l,m,n}\sqrt{\frac{2l+1}{8\pi^2}}[(1/3) \times (O_r)_{0,0,0;l,m,n} + (1/6)^{1/2}U_{2,0;l,m,n}(O_r)] \quad (25c)$$

$$C_r(\epsilon=0,\chi=90°) = K_c \sum_{l,m,n} p_{l,m,n}\sqrt{\frac{2l+1}{8\pi^2}}[(1/3) \times (O_r)_{0,0,0;l,m,n} - (1/2)U_{2,2;l,m,n}(O_r) - (1/2)(1/6)^{1/2}U_{2,0;l,m,n}(O_r)] \quad (25d)$$

When the relaxation time due to probe motion is long compared to the fluorescence lifetime, $O_r = (1/2\tau H)^r$ in eq 25. This approximation is appropriate for our application to muscle fibers.

The parameters in eq 25 are the following: the coefficients $p_{l,m,n}$ that depend on the steady-state angular distribution order parameters ($a^l_{k,q}$) and the absorption dipole moment (μ_a), the emission dipole moment (μ_e), and the matrix elements of H^r. The values for μ_a, μ_e, and some of the $a^l_{k,q}$'s can be determined from independent experimental observations. For myosin cross-bridges, μ_a and μ_e are approximately known for the fluorescent probe 1,5-IAEDANS (Mendelson et al., 1973). The steady-state order parameters for this system are dependent on the physiological state of the muscle, and some of them are also experimentally known for relaxed cross-bridges (Burghardt, 1985). Usually only the matrix elements of H^r in eq 25 are the unknowns to be determined in the time-resolved experiments.

Model Calculation for Rotational Diffusion in a Potential. When the operator H describes rotational Brownian motion in a potential, then

$$H = \sum_{i=1}^{3}[D_i L_i + u_i L_i(L_i V)] \quad (26)$$

where D_i is the rotational diffusion constant, u_i is the rotational mobility, L_i is an operator identical with the quantum mechanical orbital angular momentum operator, and V is the angular potential (Burghardt, 1985). When $u_i = D_i/kT$, where kT is the thermal energy (Landau & Lifshitz, 1959), and with the definition $f = V/2kT$, we find

$$H = \sum_{i=1}^{3} D_i[L_i + 2L_i(L_i f)] \quad (27)$$

The matrix elements of H, for use in eq 18, are calculated by using eq 4 and 10 and the relations

$$L_1 D^l_{m,n}(\Omega) = (1/2)[(l - n)(l + n + 1)]^{1/2}D^l_{m,n+1} + (1/2)[(l - n + 1)(l + n)]^{1/2}D^l_{m,n-1} \quad (28a)$$

$$L_2 D^l_{m,n}(\Omega) = (i/2)[(l - n)(l + n + 1)]^{1/2}D^l_{m,n+1} - (i/2)[(l - n + 1)(l + n)]^{1/2}D^l_{m,n-1} \quad (28b)$$

$$L_3 D^l_{m,n}(\Omega) = nD^l_{m,n}(\Omega) \quad (28c)$$

from which we find

$$H_{j',k',q';j,k,q} = \frac{8\pi^2}{2j+1}[\tfrac{1}{2}(D_1 + D_2)j(j+1) + \tfrac{1}{2}(2D_3 - D_1 - D_2)q^2]\delta_{j,j'}\delta_{k,k'}\delta_{q,q'} + \frac{2\pi^2}{2j+1}(D_1 - D_2)[(j - q)(j - q - 1)(j + q + 1)(j + q + 2)]^{1/2}\delta_{j,j'}\delta_{k,k'}\delta_{q+2,q'} + \frac{2\pi^2}{2j+1}(D_1 - D_2)[(j + q)(j + q - 1)(j - q + 1) \times (j - q + 2)]^{1/2}\delta_{j,j'}\delta_{k,k'}\delta_{q-2,q'} + \frac{8\pi^2}{2j'+1}\sum_{l,m,n} f_{l,m,n}\sqrt{\frac{2l+1}{8\pi^2}}\langle l,j,m,k|j',k'\rangle\{[(D_1 + D_2)[l(l+1) - n^2] + 2D_3(n^2 + nq)]\langle l,j,n,q|j',q'\rangle + \tfrac{1}{2}(D_1 - D_2)[(l - n + 2)(l - n + 1)(l + n - 1)(l + n)]^{1/2} \times \langle l,j,n-2,q|j',q'\rangle + \tfrac{1}{2}(D_1 - D_2)[(l - n)(l - n - 1)(l + n + 1)(l + n + 2)]^{1/2}\langle l,j,n+2,q|j',q'\rangle + (D_1 + D_2)[(l - n + 1)(l + n)(j - q) \times (j + q + 1)]^{1/2}\langle l,j,n-1,q+1|j',q'\rangle + (D_1 - D_2)[(l - n + 1)(l + n)(j - q + 1)(j + q)]^{1/2}\langle l,j,n-1,q-1|j',q'\rangle + (D_1 - D_2)[(l - n)(l + n + 1)(j - q) \times (j + q + 1)]^{1/2}\langle l,j,n+1,q+1|j',q'\rangle + (D_1 + D_2)[(l - n)(l + n + 1)(j - q + 1)(j + q)]^{1/2}\langle l,j,n+1,q-1|j',q'\rangle\} \quad (29)$$

where

$$f_{l,m,n} = \sqrt{\frac{2l+1}{8\pi^2}}\int_{\Omega_0} d\Omega D^{*l}_{m,n}(\Omega)f(\Omega) \quad (30)$$

Higher order matrix elements can be calculated from eq 29 by using the completeness relation for the Wigner rotation matrix elements such that

$$\sum_{J,m_1,m_2} \frac{2J+1}{8\pi^2} D^J_{m_1,m_2}(\Omega) D^{*J}_{m_1,m_2}(\Omega') = \delta(\Omega - \Omega') \quad (31)$$

where $\delta(\Omega - \Omega')$ is the Dirac delta function. Then, for example, the second-order matrix element, $H^2_{l',m',n';l,m,n}$, is

$$H^2_{l',m',n';l,m,n} = \sum_{J,m_1,m_2} \frac{2J+1}{8\pi^2} H_{l',m',n';J,m_1,m_2} H_{J,m_1,m_2;l,m,n} \quad (32)$$

Model Calculation for Free Rotational Diffusion. When H describes free rotational Brownian motion, then it is given by eq 27 with $f = 0$. The matrix elements of this H are derived by setting $f_{l,m,n} = 0$ in eq 29. Because of the simplicity of the free diffusion model, we have used a symbolic manipulation program (SMP) to explicitly compute $\mathcal{F}_\parallel(t)$ and $\mathcal{F}_\perp(t)$ from eq 25. We find they are given by eq 25a,b with

$$C_0(\epsilon=0,\chi=0) = C_0(\epsilon=0,\chi=90°) = K_c[\tfrac{5}{6}(K_a + K_b + K_c)/K_c + \tfrac{2}{3}(\mu_a^{-1}\mu_a^{1} + \mu_a^{0}\mu_a^{0})(\mu_e^{-1}\mu_e^{1} + \mu_e^{0}\mu_e^{0}) + \mu_a^{-1}\mu_a^{-1}\mu_e^{1}\mu_e^{1} + \mu_a^{1}\mu_a^{1}\mu_e^{-1}\mu_e^{-1} - 2\mu_a^{-1}\mu_a^{0}\mu_e^{0}\mu_e^{1} - 2\mu_a^{0}\mu_a^{1}\mu_e^{-1}\mu_e^{0}] \quad (33a)$$

and

$$C_1(\epsilon=0,\chi=0) = -\tfrac{1}{2}C_1(\epsilon=0,\chi=90°) = \tfrac{2}{15}(\tau/2)K_c\{\mu_a^{-1}\mu_a^{-1}[\mu_e^{1}\mu_e^{1}(D_1 + D_2 + 4D_3) + (\mu_e^{-1}\mu_e^{1} + \mu_e^{0}\mu_e^{0})(D_1 - D_2)] + \mu_a^{1}\mu_a^{1}[\mu_e^{-1}\mu_e^{-1}(D_1 + D_2 + 4D_3) + (\mu_e^{-1}\mu_e^{1} + \mu_e^{0}\mu_e^{0}) \times (D_1 - D_2)] + \tfrac{2}{3}(\mu_a^{-1}\mu_a^{1} + \mu_a^{0}\mu_a^{0})[(\mu_e^{-1}\mu_e^{1} + \mu_e^{0}\mu_e^{0})(3D_1 + 3D_2) + (\mu_e^{-1}\mu_e^{-1} + \mu_e^{1}\mu_e^{1})(D_1 - D_2)] + 3\mu_a^{-1}\mu_a^{0}[\mu_e^{-1}\mu_e^{0}(D_2 - D_1) - \tfrac{1}{3}\mu_e^{0}\mu_e^{1}(5D_1 + 5D_2 + 2D_3)] + 3\mu_a^{0}\mu_a^{1}[-\tfrac{1}{3}\mu_e^{-1}\mu_e^{0}(5D_1 + 5D_2 + 2D_3) + \mu_e^{0}\mu_e^{1}(D_2 - D_1)]\} \quad (33b)$$

Materials and Methods

Chemicals. ATP, ADP, P^1,P^5-di(adenosine-5′) pentaphosphate (Ap_5A), myokinase, and hexokinase were from Sigma (St. Louis, MO). 1,5-IAEDANS was from Molecular Probes (Junction City, OR). All chemicals were of analytical grade.

Solutions. Rigor solution was 80 mM potassium chloride, 5 mM magnesium chloride, 2 mM ethylene glycol bis(β-aminoethyl ether)-*N,N,N′,N′*-tetraacetic acid (EGTA), 5 mM sodium phosphate, and 0.1 mM dithiothreitol (DTT), pH 7.0.

Relaxing solution had the same composition as rigor solution except that ATP was added at 4 mM concentration.

Rigor plus calcium solution contained 0.1 or 1 mM Ca^{2+} in addition to rigor solution without EGTA.

Muscle Fibers. Rabbit psoas muscle fibers were obtained as previously described (Borejdo et al., 1979) and kept in a relaxing solution containing 50% glycerol at −15 °C for up to several weeks. Before the fibers were labeled, they were transferred to rigor solution, and one to two bundles of one to three fibers each were mounted vertically or horizontally on a 1.4 cm × 3 cm rectangular stainless-steel support made to fit diagonally in a standard fluorescence cuvette [see Figure 1 in Burghardt & Ajtai (1985)]. The fast-reacting thiol (SH-1) of the myosin cross-bridge in the fiber was labeled with 1,5-IAEDANS as described previously (Borejdo & Putnam, 1977). By this treatment, 86% of the 1,5-IAEDANS is covalently attached to SH-1 (Borejdo & Putnam, 1977; Takashi et al., 1976). Modification of SH-1 with 1,5-IAEDANS does not impair fiber contractility even when the degree of labeling is as high as 0.8 mol of fluorophore/mol of myosin (Nihei et al., 1974).

Preparation of Subfragment 1 of Myosin. Rabbit myosin was prepared by a standard method (Tonomura et al., 1966); S-1 was obtained by digesting myosin filaments with α-chymotrypsin (Weeds & Taylor, 1975). The labeling of S-1 with 1,5-IAEDANS was carried out as described by Duke et al. (1976).

Decoration of 1,5-IAEDANS-Labeled Fibers with Extrinsic Unlabeled S-1. Fibers were mounted and labeled with 1,5-IAEDANS as above. The fibers were then washed with rigor solution. The decoration of the fibers was done in rigor at 4 °C with a saturating concentration (3–4 mg/mL) of S-1 for 15 min. The fluorescence measurement was carried out without removing the unbound S-1.

Decoration of Unlabeled Fibers with Extrinsic 1,5-IAEDANS-Labeled S-1. The same procedure was used as described previously except that unbound labeled S-1 was washed out of the fibers with rigor solution immediately before the experiment.

Time-Resolved Fluorescence Measurements. The time-resolved measurements were performed on an instrument described previously (Mendelson et al., 1973; Burghardt & Thompson, 1985a). Fluorescence was excited with vertically polarized light at wavelengths <370 nm and collected (at 90°) at wavelengths >450 nm. The decay curves were collected over a time interval of <1 h. Our choice of excitation wavelength causes the excitation of two electronic transitions in the 1,5-IAEDANS molecule (Hudson & Weber, 1973) and increases the fraction of "nonspecific" emission (see Results).

We made measurements on muscle fibers in two orientational configurations. In the vertical configuration, the fiber axis is parallel to the excitation light polarization so that the depolarization curves are sensitive to rotational motions of the probes about axes other than the fiber axis. In the horizontal configuration, the excitation light polarization is perpendicular to the fiber axis, and its light propagation vector makes an angle of 45° with the fiber axis. Decay curves from the horizontal fibers are sensitive to probe motion about axes parallel to the fiber axis.

In control experiments, steady-state fluorescence polarization from 1,5-IAEDANS-labeled fibers in the vertical configuration was measured. We obtained polarization ratios identical with those measured previously from labeled fibers in rigor and relaxation (Borejdo & Putnam, 1977).

Experiments performed on relaxed fibers were done at 22 °C. Experiments on fibers in rigor were done at 4 °C.

Data Analysis. Deconvolution of the finite-width lamp pulse was done by an iterative reconvolution grid-search method (Grinvald & Steinberg, 1974; Badea & Brand, 1979). Goodness of fit was evaluated from the value of χ^2, visual inspection of the difference between experimental and theoretical curves (the residual), and visual inspection of the autocorrelation of residuals (Badea & Brand, 1979).

Decay curves corresponding to the two polarization components of the fluorescence depolarization signal in eq 25a,b were fitted by varying the fluorescence lifetime (that was identical for both curves). The amplitudes C_r, defined in eq 25c,d, were computed from the decay curves for each lifetime choice by the method outlined under Theory (eq 22–24). Every data set was well fitted by two fluorescence lifetimes.

Model Calculations. Model calculations described under Theory (eq 26–33) were performed by a symbolic manipulation

Table I: Fluorescence Lifetimes (ns) of 1,5-IAEDANS Covalently Attached to Cross-Bridges in Skeletal Muscle Fibers[a]

	relaxed		rigor	rigor + S-1	rigor + S-1
	vertical	horizontal	horizontal	horizontal	horizontal
τ_1 (ns)	2.9 ± 0.4	2.5 ± 0.8	5.4 ± 2.0	5.0 ± 2.0	6.1 ± 0.5
τ_2 (ns)	20.1 ± 0.3	19.7 ± 0.7	19.0 ± 2.0	18.0 ± 1.0	20.0 ± 0.5

[a] Shown are the means ± standard deviations of fluorescence lifetimes from fluorescence depolarization curves fitted by using the model-independent analysis with two lifetime components. The subscripts 1 and 2 correspond to the nonspecific and specific probe populations, respectively. Each number represents an average over at least four experimental curves obtained from independently prepared fibers.

Table II: Theoretical and Experimental Values for the Model-Independent Coefficients C_r[a]

		relaxed							
		vertical			horizontal				
		expt	theory a	theory b	expt	theory a	theory b	rigor horizontal	rigor + Ca^{2+} horizontal	rigor + S-1 horizontal
τ_1	$C_0(\perp)$	0.025 ± 0.006			0.06 ± 0.03			0.033 ± 0.007	0.03 ± 0.01	0.07 ± 0.03
	$C_0(\parallel)$	0.08 ± 0.03			0.10 ± 0.03			0.07 ± 0.01	0.08 ± 0.01	0.10 ± 0.03
τ_2	$C_0(\perp)$	0.25 ± 0.02	0.25	0.25	0.293 ± 0.005	0.29	0.29	0.30 ± 0.01	0.29 ± 0.01	0.30 ± 0.01
	$C_0(\parallel)$	0.50 ± 0.04	0.50	0.50	0.42 ± 0.01	0.42	0.42	0.42 ± 0.02	0.44 ± 0.02	0.40 ± 0.02
	$C_1(\perp)$	0.006 ± 0.002	0.006	0.009	0.02 ± 0.01	−0.003	0.016	0.03 ± 0.01	0.015 ± 0.003	0.02 ± 0.02
	$C_1(\parallel)$	0.019 ± 0.003	0.017	0.017	0.05 ± 0.01	0.005	0.033	0.04 ± 0.01	0.029 ± 0.004	0.04 ± 0.02
	$C_2(\perp)$	0.002 ± 0.001			0.004 ± 0.002			0.004 ± 0.002	0.002 ± 0.001	0.004 ± 0.002
	$C_2(\parallel)$	0.005 ± 0.001			0.008 ± 0.002			0.006 ± 0.001	0.004 ± 0.001	0.007 ± 0.003

[a] The experimental C_r's were determined by using fluorescence depolarization curves from 1,5-IAEDANS-labeled cross-bridges in muscle fibers. Shown are the means ± standard deviations for C_r. τ_1 and τ_2 and the accompanying C_r's correspond to the nonspecific and specific probe populations, respectively. Each experimental number represents an average over at least four experimental curves obtained from independently prepared fibers. For relaxed fibers, coefficients C_r in theory a are obtained by using the rotational diffusion constants $D_1 = D_2 = 7.5 \times 10^5\ s^{-1}$ and $D_3 = 18 \times 10^5\ s^{-1}$ and the order parameters $a^0_{0,0} = (1/8\pi^2)^{1/2}$, $a^2_{0,0} = 0.06$, $a^2_{0,2} = a^2_{0,-2} = 0.002$, and $a^4_{0,0} = 0.02$. Theory b is obtained by using the rotational diffusion constants $D_1 = D_2 = 2.5 \times 10^5\ s^{-1}$ and $D_3 = 6 \times 10^5\ s^{-1}$, the order parameters used in theory a, and the rank 6 order parameters $a^6_{0,0} = -0.05$ and $a^6_{6,0} = a^6_{6,0} = -0.025$. These models are discussed under Results. Any experimental C_r not explicitly appearing in the table is ≈0. No theoretical calculation of C_r for $r > 1$ or for the emission from the nonspecific population was attempted.

program, SMP (Inference Corp., Los Angeles, CA). SMP is installed on a VAX 750 computer (Digital Equipment Corp., Marlboro, MA) and performs explicit symbolic computation. SMP was used to compute eq 25, using the model in eq 26, in terms of unknowns that were later specified.

Results

The fluorescence lifetimes, determined from vertical and horizontal fibers in rigor and relaxation, are summarized in Table I. All of the data were fitted with two-exponential decays. The shorter lifetime emission is attributed to nonspecifically bound probes residing in the muscle fiber on sites other than SH-1 on the cross-bridge [~14% of the total number of probes; see Borejdo & Putnam (1977)] and to a second electronic transition present in 1,5-IAEDANS at excitation wavelengths <370 nm (Hudson & Weber, 1973). Previous lifetime studies of 1,5-IAEDANS-labeled S-1 in solution, where the specificity of the probe is very high, indicate that the longer lifetime is from probes bound to SH-1 (Nihei et al., 1974).

The number of terms of the series in eq 23 that contribute significantly to the fluorescence depolarization signal is determined by the rapidity and nature of the rotational motion of the probes. If the fluorescence depolarization signal from immobilized probes is measured, $C_0 > 0$ and $C_r = 0$ for $r > 0$. Higher order components ($r > 0$) will contribute when any rotational motion is present, but for every motion, there will be a maximum value of r (r_{max}) such that $C_r \approx 0$ when $r > r_{max}$.

In our data-fitting procedure, rotational motion can be attributed to each of the fluorescence lifetime components present in the depolarization signal. We found that in every case the contribution to the fluorescence depolarization signal from the shorter lifetime component (component 1 in Table I) was characterized by $C_0 > 0$ and $C_r \approx 0$ for all $r > 0$. This result indicates there was no detectable rotational motion in the nonspecific fluorescent emission. The longer lifetime component (component 2 in Table I) indicates the presence of rotational motion that was always characterized by a few of the lowest order C_r's being finite and the rest zero. In every case, $r_{max} < 3$. The results of these analyses are summarized in Table II and are discussed in detail below.

Relaxed Muscle Fibers in the Vertical Configuration. The model of rotational diffusion in a potential is appropriate for application to relaxed cross-bridges in muscle fibers. In this state, the cross-bridges are not attached to actin and are confined in a mildly restrictive angular potential that is probably imposed by the interaction of the cross-bridge with the thick filament (Burghardt et al., 1984). Using eq 20 with available steady-state fluorescence polarization data (Wilson & Mendelson, 1983), we have shown previously that, in the vertical fiber configuration, $P(\Omega,t\rightarrow\infty)$ is described by the order parameters $a^0_{0,0} = (1/8\pi^2)^{1/2}$, $a^2_{0,0} = 0.06$, $a^2_{0,2} = a^2_{0,-2} = 0.002$, and $a^4_{0,0} = 0.02$ (Burghardt, 1985). Order parameters of rank >4 are not detectable by using the steady-state fluorescence polarization technique (Burghardt, 1984). The coefficients $f_{l,m,n}$ defined in eq 30 are computed from the order parameters $a^l_{m,n}$ via the relation

$$P(\Omega,t\rightarrow\infty) = c \exp(-2f) \qquad (34)$$

where c is a normalization constant and by eq 20.

Previously, time-resolved fluorescence anisotropy decay (TRFAD) measurements performed on S-1 labeled with 1,5-IAEDANS and bulk-dissolved have given some indication of the orientation of the probe relative to the hydrodynamic principal axis frame of the protein fragment (Mendelson et al., 1973). From these studies, it is indicated that if

$$\mu_a = (\sin\theta_a \cos\phi_a, \sin\theta_a \sin\phi_a, \cos\theta_a) \qquad (35a)$$

$$\mu_e = (\sin\theta_e \cos\phi_e, \sin\theta_e \sin\phi_e, \cos\theta_e) \qquad (35b)$$

and the hydrodynamic principal frame (our molecular frame) has its z axis along the long dimension of the ellipsoid of revolution shape given to S-1, then θ_a and θ_e are <40° and $\phi_a = \phi_e = 0$. Steady-state fluorescence polarization experiments

on random immobilized 1,5-IAEDANS attached to S-1 indicate the angle between μ_a and μ_e to be $\sim 37°$ when the excitation wavelength is 350 nm and emission is collected at 476 nm. Consistent with our present data and these constraints is our choice of $\theta_a = 0$, $\theta_e = 37°$, and $\phi_a = \phi_e = 0$.

These choices for μ_a and μ_e, and $a^l_{m,n}$, leave the diffusion constants, D_i, as the free parameters remaining in the model. If we assume S-1 is an ellipsoid of revolution with an axial ratio of 3.5, then our previous conventional analysis of these data (Burghardt & Thompson, 1985a) suggests $D_1 = D_2 = 1.25 \times 10^5$ s^{-1} and $D_3 = 3.0 \times 10^5$ s^{-1}. We have computed the model-independent coefficients, C_r defined in eq 18b, using the model with the choices for μ_a, μ_e, and $a^l_{m,n}$ quoted above (we call this model a), for various values of D_i. We have compared these theoretical values for C_r with the experimental values computed from the time-resolved fluorescence depolarization curves for relaxed fibers in the vertical configuration at room temperature. The theoretical and experimental values for C_r are summarized in Table II. We find that the choices $D_1 = D_2 = 7.5 \times 10^5$ s^{-1} and $D_3 = 1.8 \times 10^6$ s^{-1} lead to theoretical values of C_r, listed under the heading theory a in Table II that agree with the experimental estimates of C_r to within experimental error. These values for D_i are 6 times larger than those estimated by the previous conventional analysis.

Alternatively, we have calculated C_r using a model that includes order parameters of rank 6 in the steady-state angular distribution; we call this model b. The rank 6 order parameters and the diffusion constants are the free variables in the model calculation of C_r. Model b is proposed because it is consistent with data from both vertical and horizontal fibers (see next section). The data from horizontal fibers impose an additional constraint on the model. Model b is discussed in more detail in the next section on horizontal fibers. For the choices $D_1 = D_2 = 2.5 \times 10^5$ s^{-1}, $D_3 = 6 \times 10^5$ s^{-1}, $a^6_{0,0} = -0.05$, and $a^6_{6,0} = a^6_{-6,0} = -0.025$, we find the theoretical values for C_r that are listed under the heading theory b in Table II. These values for D_i are 2 times larger than those estimated by the conventional analysis. The theoretical values for the C_r's generated by using model b are not as close to the experimental values for the vertical fibers as those generated from model a. Model b is, however, the more reliable since it is consistent with more of the known constraints.

Our estimates of $a^6_{0,0}$ and $a^6_{6,0}$ are independent of the estimates of the values of the other order parameters. The steady-state fluorescence polarization measurements responsible for the estimates of the order parameters of rank ≤ 4 are independent of the values for $a^l_{m,n}$ when $l > 4$. Thus, we are correct in allowing $a^6_{m,n}$ to vary freely while the lower rank order parameters are held constant when the time-resolved data are fitted.

Relaxed Muscle Fibers in the Horizontal Configuration. In the horizontal configuration, the cross-bridge order parameters, $a'^l_{m,n}$, are derived from the vertical fiber order parameters by using the transformation (Burghardt, 1985)

$$a'^l_{m,n} = \sum_k a^l_{k,n} D^l_{k,m}(\alpha = -\pi/4, \beta = \pi/2, \gamma = 0) \quad (36)$$

A similar relationship holds for the coefficients, $f'_{l,m,n}$. We have computed C_r for horizontal fibers using model a, the diffusion constants $D_1 = D_2 = 7.5 \times 10^5$ s^{-1} and $D_3 = 1.8 \times 10^6$ s^{-1}, the values for $a'^l_{m,n}$ and $f'_{l,m,n}$ computed by using eq 36, and μ_a and μ_e (which are independent of the fiber configuration or physiological state). The results of this computation, summarized in Table II under the heading theory a, show that the theory disagrees with what is observed. The disagreement cannot be accounted for by altering D_i since this cannot alter the sign of $C_1(\perp)$. The difference between theory and experiment indicates that the proposed steady-state angular distribution of cross-bridges in model a does not account for the time-resolved fluorescence polarization data from horizontal fibers. Model a predicts that for the horizontal configuration the cross-bridges move relatively freely. This prediction is indicated by comparison of coefficients $C_1(\perp)$ and $C_1(\parallel)$, calculated from eq 33b for the free diffusion case, to those from model a. This result is reasonable since model a allows the cross-bridges to move freely in their α degree of freedom; i.e., $P(\Omega, t \rightarrow \infty)$ is independent of α. We observe this effect now since the horizontal fiber configuration is sensitive to α dependence in $P(\Omega, t \rightarrow \infty)$ while the vertical configuration is comparatively insensitive to α. Our experimental results therefore suggest that a more correct model is one with the proper α dependence in the steady-state angular distribution. We call this degree of freedom in the cross-bridge its azimuthal degree of freedom.

The proposed new model (model b that we introduced in the previous section) incorporates 6-fold azimuthal symmetry in the steady-state angular distribution since each myosin filament is known to be in this arrangement in a two-dimensional lattice with actin filaments. Real muscle fibers contain many sarcomeres, and our experiments are performed on long segments of single fibers; consequently, the 6-fold azimuthal symmetry is not expected to persist throughout the sample. The steady-state angular distribution averaged over the entire sample is probably independent of α even though individual cross-bridges may feel an α-dependent potential. A method for modeling this system is to calculate the fluorescent signal from one sarcomere with 6-fold symmetry and azimuthal angle α_1 relative to a plane containing the fiber axis. The order parameters for such a sarcomere are, from eq 36

$$a'^l_{m,n} = \sum_k a^l_{k,n} D^l_{k,m}(\alpha = \alpha_1 - \pi/4, \beta = \pi/2, \gamma = 0) \quad (37)$$

A similar relationship holds for $f'_{l,m,n}$. We then integrate over all sarcomeres (i.e., over α_1 with $0 \leq \alpha_1 \leq 2\pi$) to obtain the total signal. Terms in the total fluorescence signal that depend on α_1 average to zero after integration. Terms that contain products $a^l_{m,n} f_{l,-m,k}$ cancel their α_1 dependence and contribute to the total signal.

The order parameters that represent the 6-fold azimuthal symmetry of the fiber are $a^6_{0,0}$ and $a^6_{6,0} = a^6_{-6,0}$. These order parameters with $a^6_{0,0} \propto {}^1/_2$ and $a^6_{6,0} \propto {}^1/_4$ would correspond to a steady-state angular distribution for a single sarcomere that is proportional to $\cos^2(3\alpha_1)$. The values for the order parameters, diffusion constants, and dipole moments are identical with the choices in model b for the vertical fiber. The results of the computations with model b are shown in Table II under the heading theory b. We find we can now qualitatively imitate the observed results for the horizontal relaxed fibers with our theory. However, we emphasize that the agreement between experiment and theory is only qualitative since no choice of the diffusion constants D_i places the theoretical results within the experimental uncertainty of all of the C_r's.

An interesting new feature of the proposed steady-state angular distribution is introduced by the addition of the rank 6 order parameters. Shown in Figure 1 is a comparison of the two steady-state distributions used in models a and b. Both distributions are even on the interval $0 \leq \beta \leq \pi$, where β is the polar angle relative to the fiber axis, so that the distributions are necessarily symmetrical about $\beta = \pi/2$. The steady-state distribution in model b has peaks near $\beta = 0$ and

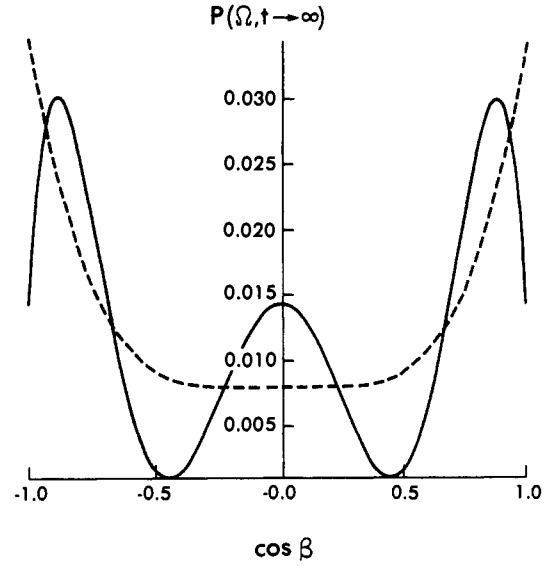

FIGURE 1: Relaxed cross-bridge steady-state angular distribution as a function of cos β at $\alpha = \gamma = 0$. The dashed line corresponds to the distribution of a model with order parameters $a^0_{0,0} = (1/8\pi^2)^{1/2}$, $a^2_{0,0} = 0.06$, $a^2_{0,2} = a^2_{0,-2} = 0.002$, and $a^4_{0,0} = 0.02$ (model a). The solid line corresponds to the distribution of a model with order parameters identical with model a with $a^6_{0,0} = -0.05$ and $a^6_{-6,0} = a^6_{6,0} = -0.025$ (model b). All distributions are symmetrical with respect to $\beta = \pi/2$ (since only order parameters with even rank are included). The model b distribution is bimodal, indicating two preferred β orientations for relaxed cross-bridges.

$\pi/2$, indicating a bimodal distribution in β. Model a does not have a bimodal feature.

The observed time-resolved results are equivalent, to first order in time, to a polarization anisotropy relaxation time of ~200 ns. This is the relaxation time reported earlier when this quantity is computed by conventional analysis routines (Burghardt & Thompson, 1985a).

Muscle Fibers in Rigor in the Horizontal Configuration. Model calculations for cross-bridges in rigor have not been attempted. We report here the experimental determination of C_r from time-resolved fluorescence depolarization measurements.

We have shown previously that rigor cross-bridges show rapid rotational motion that is not dependent on temperature when 4 °C < T < 25 °C. This rapid motion is equivalent, to first order in time, to a polarization anisotropy relaxation time of ~200 ns. These results were obtained by using conventional analysis routines (Burghardt & Thompson, 1985a; Burghardt & Ajtai, 1985).

We also find that the rapidity of the rigor corss-bridge rotational motion is not affected by the presence of calcium (at concentrations of 0.1–1.0 mM) or when the actin filaments are decorated with saturating concentrations of extrinsic unlabeled S-1. All of the horizontal rigor fiber data are summarized in Table II. Typical time-resolved fluorescence depolarization curves and their theoretical fits, for rigor cross-bridges, are shown in Figure 2.

The time-resolved fluorescence depolarization from unlabeled fibers in rigor that were decorated with 1,5-IAEDANS-labeled S-1 showed the actin-attached S-1 moved with the same rapidity as the rigor cross-bridge.

Discussion

We have described a model-independent treatment of time-dependent rotational motion of molecules in biological assemblies. In this treatment, the time development of the angular distribution function is obtained by using a time-development operator that is expanded in orthonormal functions of time. The expansion coefficients are terms with increasing order in the differential operator that describes the physical processes that cause molecular rotational motion. Matrix elements of the expansion coefficients are uniquely determined from experimental data by a method we have developed here.

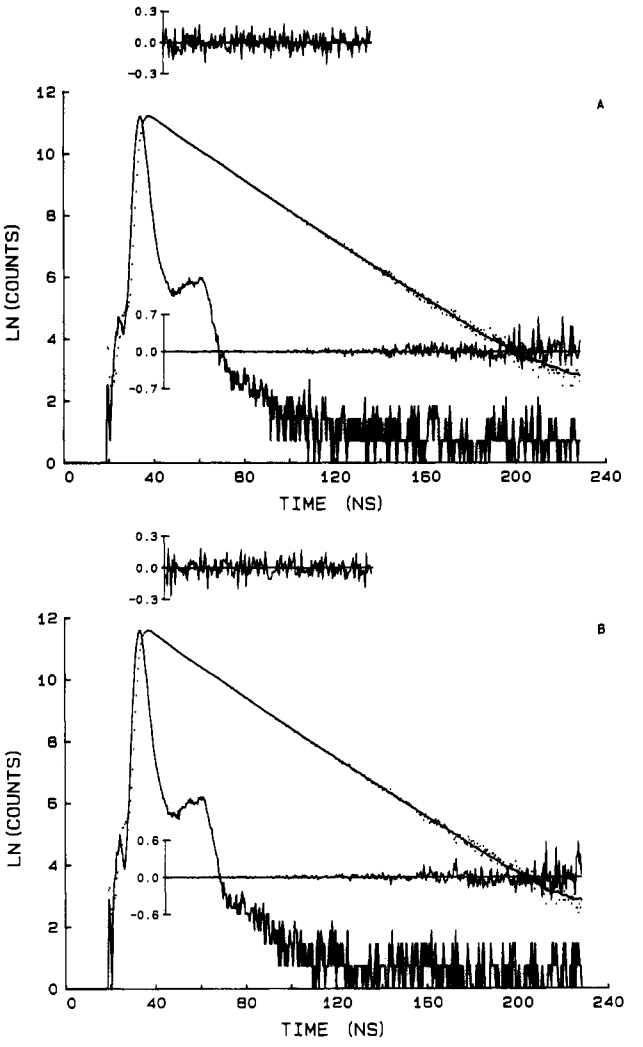

FIGURE 2: Time-resolved fluorescence depolarization curves from rigor fibers in the horizontal configuration. $\mathcal{F}_\perp$ (A) and $\mathcal{F}_\parallel$ (B) (see eq 25) are shown as a function of time. The solid line is the theoretical fit. The lamp profile, the residuals, and the autocorrelation of residuals are also shown. The latter two curves indicate the goodness of the theoretical fit.

The model-independent method allows the quantitative analysis of a time-dependent experiment in terms of elementary quantities of the system without a model. If a model is chosen, it can be conveniently handled within the model-independent theory. A model is used to compute the theoretical value of the matrix elements measured experimentally. We have demonstrated the power of our method by making model calculations for a macromolecule undergoing rotational diffusion in a three-dimensional angular potential. This is the first time this calculation has been completed exactly on a fully three-dimensional angular potential.

We have applied this formalism to the motion of myosin cross-bridges and actin filaments in the actomyosin complex in muscle fibers that have the fluorescent probe 1,5-IAEDANS specifically attached to the cross-bridge. The rapidity of rotational motion of cross-bridges in relaxed muscle fibers in the vertical configuration has been measured and treated theoretically by a conventional formalism previously (Burghardt

& Thompson, 1985a). We have shown here that our model-independent formalism, used with the rotational diffusion in a potential model, is in rather close quantitative agreement with the conventional formalism with regard to the determination of the rotational diffusion constants of the cross-bridges. The small difference in results is probably due to features of the model-independent analysis that are improvements over the conventional analysis. These improvements are the following: (1) the analysis of $\mathcal{F}_{\parallel}(t)$ and $\mathcal{F}_{\perp}(t)$ independently rather than the analysis of the anisotropy which is a complicated function of relaxation times and fluorescence lifetimes in ordered systems; (2) the ability to separate the motions attributed to different lifetimes in the fluorescence decay (Burghardt, 1985; Burghardt & Thompson, 1985a). Other quantitative findings for relaxed cross-bridges, such as the time zero anisotropy, are identical for the two methods of analysis.

Relaxed cross-bridges in the horizontal configuration have not previously been treated theoretically because of the complication of the conventional theory for a three-dimensional potential, in the rotational diffusion in a potential model (Burghardt, 1985). The present formalism successfully handles this problem and in so doing adds an additional constraint to the free parameters in the model. This constraint allows the determination of previously ignored order parameters of rank 6 in the proposed cross-bridge steady-state angular distribution. These order parameters are not measurable by steady-state methods.

The newly incorporated order parameters for relaxed cross-bridges introduce a distinctive bimodal feature in the proposed cross-bridge steady-state angular distribution in the polar angle. The presence of a bimodal cross-bridge distribution in rigor fibers has been reported earlier (Burghardt & Thompson, 1985b; Ajtai & Burghardt, 1986). This feature now also appears to be present in relaxed fibers, suggesting it is an intrinsic property of the thick filament.

The rapidity of rotational motion of rigor cross-bridges in muscle fibers in the horizontal configuration has also been reported previously (Burghardt & Thompson, 1985a; Burghardt & Ajtai, 1985). In that work, we suggested that the cross-bridge motion may be the result of actin filament motion. We have attempted to investigate this possibility by measuring the rapidity of the rigor cross-bridge in the presence of actin-perturbing agents such as Ca^{2+} and extrinsic S-1. The effect of Ca^{2+} or S-1 on F-actin motion in the 10^{-6}–10^{-3}-s time domain is well established (Mihashi et al., 1983; Thomas et al., 1979; Yanagida et al., 1984; Oosawa, 1980). However, earlier reports disagree whether or not nanosecond motion is present in F-actin (Mihashi et al., 1983; Thomas et al., 1979). If we assume that the presence of Ca^{2+} or S-1 perturbs the rapidity of actin motion in intact fibers in the nanosecond time domain, then the present results, that these agents have no effect on the rapidity of rigor cross-bridge motion in the nanosecond time domain (see Table II), suggest the motion is from flexibility within the cross-bridge. However, our previous studies indicating that (1) there is only much slower motion of relaxed cross-bridges under identical conditions (horizontal configuration, at $T = 4$ °C) and (2) there is no nanosecond motion of rigor cross-bridges in the vertical configuration at room temperature diminish the probability of this explanation [see Burghardt & Thompson (1985a), Burghardt & Ajtai (1985), and similar findings using the model-independent analysis]. The most plausible explanation is that the rigor cross-bridge is moving as a result of actin filament rotation about the fiber axis that is not affected by calcium or S-1 in the intact fiber system. These results pertain only to motions faster than a few thousand nanoseconds. The lack of an actin filament perturbation due to Ca^{2+} and S-1 may be because we used intact fibers and not reconstituted systems as were used in the previous studies (Mihashi et al., 1983; Thomas et al., 1979).

The application of our model-independent analysis to the motion of rigor cross-bridges in horizontal muscle fibers is a good demonstration of the analysis technique. Clearly, the conventional methods of data analysis would have produced the same qualitative results; however, the conventional methods are based on a single model so that the quantitative results derived from it are less generally applicable. With the data summarized in terms of C_r, any model can be applied. The apparent motion of the actomyosin complex in rigor fibers will need a model that accounts for properties of the actin filament as well as the myosin cross-bridge.

The calculation based on the rotation in a potential model, that was used in the study of relaxed cross-bridges, was performed with the aid of a symbolic manipulation program. This program proved to be very useful in that the computation of the fluorescence signal from eq 25, using the initial condition and the model to determine H, is done in a few lines of symbolic programming language. The explicit symbolic expressions for $F_{\parallel}(t)$ and $F_{\perp}(t)$, where parameters D_i, $a^l_{m,n}$, μ_a, μ_e, and $f_{l,m,n}$ that change from experiment to experiment are included symbolically, are stored in a file that can be recalled and used repeatedly to compute numerical values for $F_{\parallel}$ and $F_{\perp}$. The most complex calculation performed was for the rotational diffusion in a three-dimensional potential model. SMP on a VAX 750 took 48 h to do this symbolic calculation. Once completed, this explicit expression is used to compute numerical results within a few seconds.

ACKNOWLEDGMENTS

We thank Paul Curmi and Manuel Morales for valuable scientific discussions and Joan Junkin for help in typing the manuscript.

APPENDIX

In eq 12–18, we describe a procedure to determine the coefficients of the expansion in time of the relaxation curve. The assumption that $^1/_2\tau H < 1$, important in the derivation of eq 13, is not essential to the model-independent approach. The procedure in the text is part of a more general method for obtaining the coefficients of the relaxation curve using Laplace transforms. The general method can be used for any fluorescence lifetime. Below we briefly outline the more general procedure.

If $R(t)$ is the relaxation curve, not dependent on the fluorescence lifetime, then

$$R(t) = \sum_{i,j} a_{i,j} \int_{\Omega_0} d\Omega D_i^*(\Omega) \exp(-Ht) D_j(\Omega) \qquad \text{(A1)}$$

where $a_{i,j}$ is some constant and $D_i(\Omega)$ is a Wigner matrix element. Equation A1 is Laplace-transformed to give

$$\alpha \int_0^\infty dt \exp(-\alpha t) R(t) = R(0) - \sum_{i,j} a_{i,j} \int_{\Omega_0} d\Omega D_i^*(\Omega) \frac{H/\alpha}{1 + H/\alpha} D_j(\Omega) \qquad \text{(A2)}$$

With eq A2 and an appropriate choice for the positive, real constant α (a choice that makes H/α small), we can determine the lowest order (in H) matrix element from $R(t)$. This is what must be done when $\tau H > 2$. In eq 12–18, we have used $1/\tau$

as α in eq A2 since, for our system, τ is known to satisfy the requirement that $\tau H \ll 1$.

Registry No. 1,5-IAEDANS, 36930-63-9.

REFERENCES

Abramowitz, M., & Stegun, I., Eds. (1972) *Handbook of Mathematical Functions with Formulas, Graphs, and Mathematical Tables*, pp 773–802, U.S. Government Printing Office, Washington, DC.

Ajtai, K., & Burghardt, T. P. (1986) *Biochemistry* (in press).

Axelrod, D. (1979) *Biophys. J. 26*, 557–573.

Badea, M., & Brand, L. (1979) *Methods Enzymol. 61*, 378–425.

Borejdo, J., & Putnam, S. (1977) *Biochim. Biophys. Acta 459*, 578–595.

Borejdo, J., Putnam, S., & Morales, M. F. (1979) *Proc. Natl. Acad. Sci. U.S.A. 76*, 6346–6350.

Borejdo, J., Assulin, O., Ando, T., & Putnam, S. (1982) *J. Mol. Biol. 158*, 391–414.

Burghardt, T. P. (1984) *Biopolymers 23*, 2383–2406.

Burghardt, T. P. (1985) *Biophys. J. 48*, 623–631.

Burghardt, T. P., & Thompson, N. L. (1984) *Biophys. J. 46*, 729–738.

Burghardt, T. P., & Ajtai, K. (1985) *Proc. Natl. Acad. Sci. U.S.A. 82*, 8478–8482.

Burghardt, T. P., & Thompson, N. L. (1985a) *Biochemistry 24*, 3731–3735.

Burghardt, T. P., & Thompson, N. L. (1985b) *Biophys. J. 48*, 401–409.

Burghardt, T. P., Tidswell, M., & Borejdo, J. (1984) *J. Muscle Res. Cell Motil. 5*, 657–663.

Chuang, T. J., & Eisenthal, K. B. (1972) *J. Chem. Phys. 57*, 5094–5097.

Davydov, A. S. (1963) *Quantum Mechanics*, pp 145–169, NEO Press, Ann Arbor, MI.

Duke, J., Takashi, R., Ue, K., & Morales, M. F. (1976) *Proc. Natl. Acad. Sci. U.S.A. 73*, 302–306.

Ehrenberg, M., & Rigler, R. (1972) *Chem. Phys. Lett. 14*, 539–544.

Favro, L. D. (1960) *Phys. Rev. 119*, 53–62.

Grinvald, A., & Steinberg, J. Z. (1974) *Anal. Biochem. 59*, 583–598.

Hudson, E. N., & Weber, G. (1973) *Biochemistry 12*, 4154–4161.

Kinosita, K., Kawato, S., & Ikegami, A. (1977) *Biophys. J. 20*, 289–305.

Landau, L. D., & Lifshitz, E. M. (1959) *Fluid Mechanics*, p 228, Pergamon Press, Elmsford, NY.

McCalley, R. C., Shimshick, E. J., & McConnell, H. M. (1972) *Chem. Phys. Lett. 13*, 115–119.

Mendelson, R. A., Morales, M. F., & Botts, J. (1973) *Biochemistry 12*, 2250–2255.

Mihashi, K., Yoshimura, H., & Nishio, T. (1983) in *Actin: Structure and Function in Muscle and Non-Muscle Cells* (dos Remedios, C. G., & Barden, J. A., Eds.) Chapter 10, pp 81–88, Academic Press, New York.

Oosawa, F. (1980) *Biophys. Chem. 11*, 443–446.

Polnaszek, C. F., Bruno, G. V., & Freed, J. H. (1973) *J. Chem. Phys. 58*, 3185–3199.

Szabo, A. (1980) *J. Chem. Phys. 72*, 4620–4626.

Takashi, R., Duke, J., Ue, K., & Morales, M. F. (1976) *Arch. Biochem. Biophys. 175*, 279–283.

Thomas, D. D., Siedel, J. C., & Gergely, J. (1979) *J. Mol. Biol. 132*, 257–273.

Tonomura, Y., Appel, P., & Morales, M. F. (1966) *Biochemistry 5*, 515–521.

Weeds, A. G., & Taylor, R. S. (1975) *Nature (London) 257*, 54–56.

Wilson, M. G. A., & Mendelson, R. A. (1983) *J. Muscle Res. Cell Motil. 4*, 671–693.

Yanagida, T., Nakase, M., Nishiyama, K., & Oosawa, F. (1984) *Nature (London) 307*, 58–60.

Zannoni, C., Arcioni, A., & Cavatorta, P. (1983) *Chem. Phys. Lipids 32*, 179–250.